SDC-92-262

SDC
SOLENOIDAL DETECTOR NOTES

SCINTILLATING FIBER OUTER TRACKING DETECTOR

May 6, 1992

R. Ruchti
University of Notre Dame

SCINTILLATING FIBER OUTER TRACKING DETECTOR

Fiber Tracking Group (FTG)

B.Abbot[k], D.Adams[l], M.Adams[c], E.Anderson[m], T.Armstrong[i], M.Atac[a,b], A.Baumbaugh[b], B.Baumbaugh[g], P. Besser[n], M.Binkley[b], F.Bird[o], J.Bishop[g], N.Biswas[g], A.D.Bross[b], C.Buchanan[a], N.Cason[g], R.Chaney[p], D.Chrisman[a], D.Cline[a], C. Collins[o], M.Corcoran[l], R.Davies[k], J.Elias[b], E.Fenyves[p], D.Finley[b], G.W.Foster[b], R. Fox[o], H.Goldberg[c], H.Hammack[p], A.Hasan[i], M. Hechler[o], S.Heppelmann[i], K.Hess[o], J.Jaques[g], J.Kauffman[j], R.Kehoe[g], C.Kelley[e], M. Kelly[g], C.Kennedy[m], V.Kenney[g], R.Kephart[b], D.Koltick[k], J.Kolonko[a], K.Kondo[q], J.Kubic[a], R.A.Lewis[i], R.Leitch[h], J.LoSecco[g], B.Lowery[p], J.Marchant[g], R.McCutcheon[m], R.McIlwain[k], S.Margulies[c], H.Mendez[c], F.Miere[d], H.Miettenen[l], R.Moore[i], R.J.Mountain[g], B.Oh[i], J.Orgeron[p], H.Paik[d], J.Park[a], J.Passaneau[i], K.Pennington[o], M.Petroff[m], J. Piles[o], A.Pla-Dalmau[b], C.Rivetta[b], R.Ruchti[g], R.Scalise[i], J.Schmitz[k], W.Shephard[g], E.Shibata[k], J.Skeens[l], G.A.Smith[i], J.Solomon[c], K.Takikawa[q], C. Talmadge[k], T.Thurston[o], S.Tkaczyk[b], W.Toothacker[i], Balamurali V[g], D.Vandergriff[h], K.Vasavada[d], R.Wagner[b],, M.Wayne[g], and J.Whitmore[i]

University of California at Los Angeles[a]
Fermi National Accelerator Laboratory[b]
University of Illinois at Chicago[c]
Indiana University - Purdue University at Indianapolis[d]
Massachusetts College of Pharmacy and Allied Health Sciences[e]
University of Notre Dame[g]
Oak Ridge National Laboratory[h]
Pennsylvania State University[i]
Philadelphia College of Pharmacy and Science[j]
Purdue University[k]
Rice University[l]
Rockwell International, Electro-Optical Center[m]
Rockwell International, Science Center[n]
Superconducting Super Collider Laboratory[o]
University of Texas at Dallas[p]
Tsukuba University[q]

R. RUCHTI
NOTRE DAME
5-6-92

DESIGN STRATEGY

- ALL CYLINDRICAL GEOMETRY $0 \leq |\eta| \leq 2.3$

  UNIFORMITY OF COVERAGE FOR

  TRACKING
  TRIGGERING
  MECHANICAL SIMPLICITY

  INNER LAYERS FOR TRIGGERING AT LEVEL 1.

  OUTER LAYERS FOR MOMENTUM RESOLUTION

- EXPLOITS: INTRINSICALLY PROMPT RESPONSE OF SCINTILLATOR TO BE SENSITIVE TO INDIVIDUAL BEAM CROSSINGS

  HIGH GRANULARITY/LOW OCCUPANCY TO PROVIDE OPERATION TO 10^{34} LUMINOSITY

DESIGN CONCEPT

- SCINTILLATING FIBERS OF
  - 925 μm DIAMETER
  - PS/PTP/3HF (STANDARD MIX)
  - $\lambda \sim 530$ nm
  - (BICRON & KURARAY)
- WAVEGUIDE FIBERS OF
  - 1mm DIAMETER
  - PS ONLY (STANDARD)
  - (BICRON & KURARAY)
- PHOTODETECTORS:
  - VISIBLE LIGHT PHOTON COUNTERS (VLPC)
  - QE ~ 80% AT 565 nm.
  - OPERATE CRYOGENICALLY (6-9 K)
- MECHANICAL:
  - FIBERS FORMED INTO COHERENT RIBBONS
  - RIBBONS PLACED ON STABLE-BASE CYLINDERS OF CARBON FILAMENT/ ROHACELL STRUCTURE
  - SYSTEM IS HELD AND SUPPORTED FROM END RINGS
  - CRYOSTATS FOR VLPCs ARE PLACED OUTSIDE OF THE CALORIMETRY
- TRIGGER/DAQ:
  - OUTPUT IS DIGITAL
  - LEVEL 1 TRIGGERING IMPOSED IN ASIC TECHNOLOGY

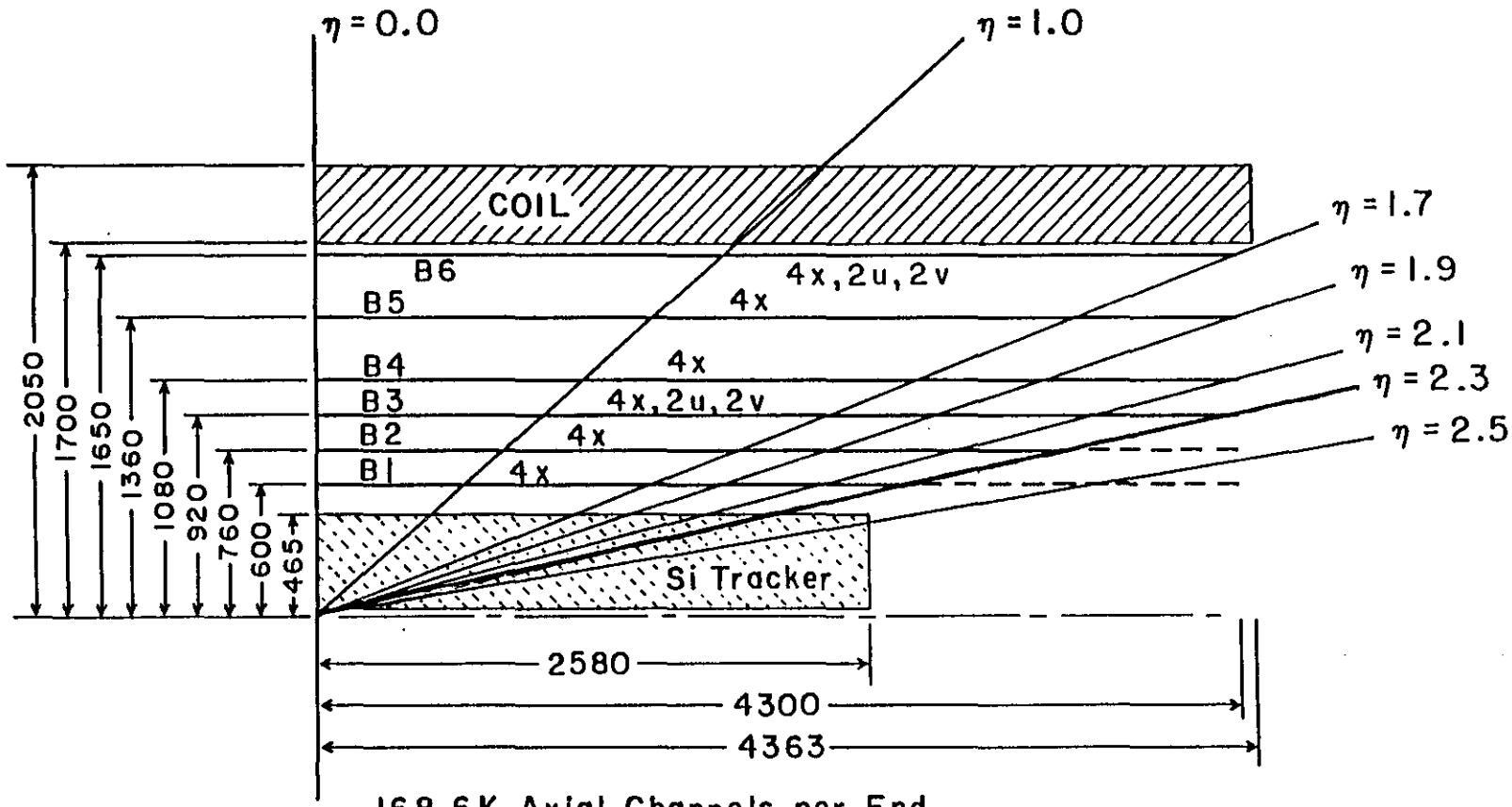

168.6 K Axial Channels per End
68.0 K Stereo Channels per End
473.2 K Total Channel Count

Table 4-21
Parameters and characteristics of the superlayers of the scintillating fiber tracker.

Radial location (cm)	Fiber layers x=axial u=stereo v=stereo	Fiber channels per end	Scifi length for axial fibers (m)	$\Delta\eta$ coverage	Wave-guide length (m)	Total fiber length (m)	Expected mean no. of photo-electrons detected for 925 μm diam. (at $\eta = 0$)
60	$2x, 2x$	15.9K	3.00	2.3	6.93	9.93	4.6
76	$2x, 2x$	20.1K	3.65	2.3	6.12	9.77	4.6
92	$2x, 2x$	24.4K					
	$2u, 2v$	24.4K	4.30	2.3	5.31	9.61	4.5
108	$2x, 2x$	28.6K	4.30	2.1	5.15	9.45	4.6
136	$2x, 2x$	36.0K	4.30	1.9	4.87	9.17	4.7
165	$2x, 2x$	43.6K	4.30	1.7	4.58	8.88	4.9
	$2u, 2v$	43.6K					

TOTAL 473.2K

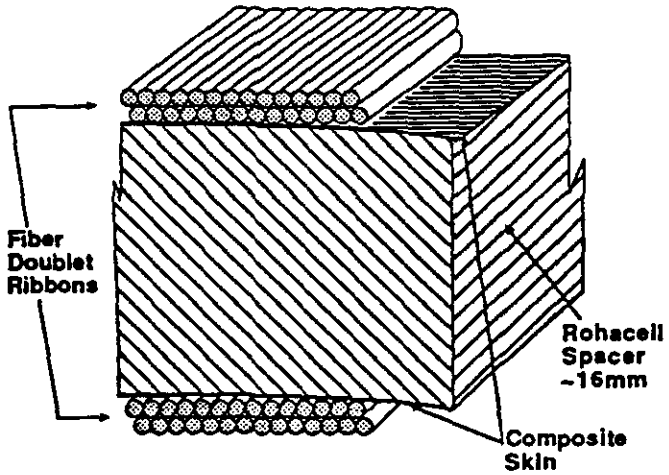

FIG. 4-58. Schematic of a superlayer having axial fiber doublet ribbons mounted on the inner and outer surfaces of a support cylinder.

Table 4-23
Average occupancies at SSC design luminosity.

Superlayer	Radius (cm)	$\Delta\eta$ coverage	Occupancy
B1	60.0	2.3	0.017
B2	76.0	2.3	0.013
B3	92.0	2.3	0.012
B4	108.0	2.1	0.006
B5	136.0	1.9	0.003
B6	165.0	1.7	0.002

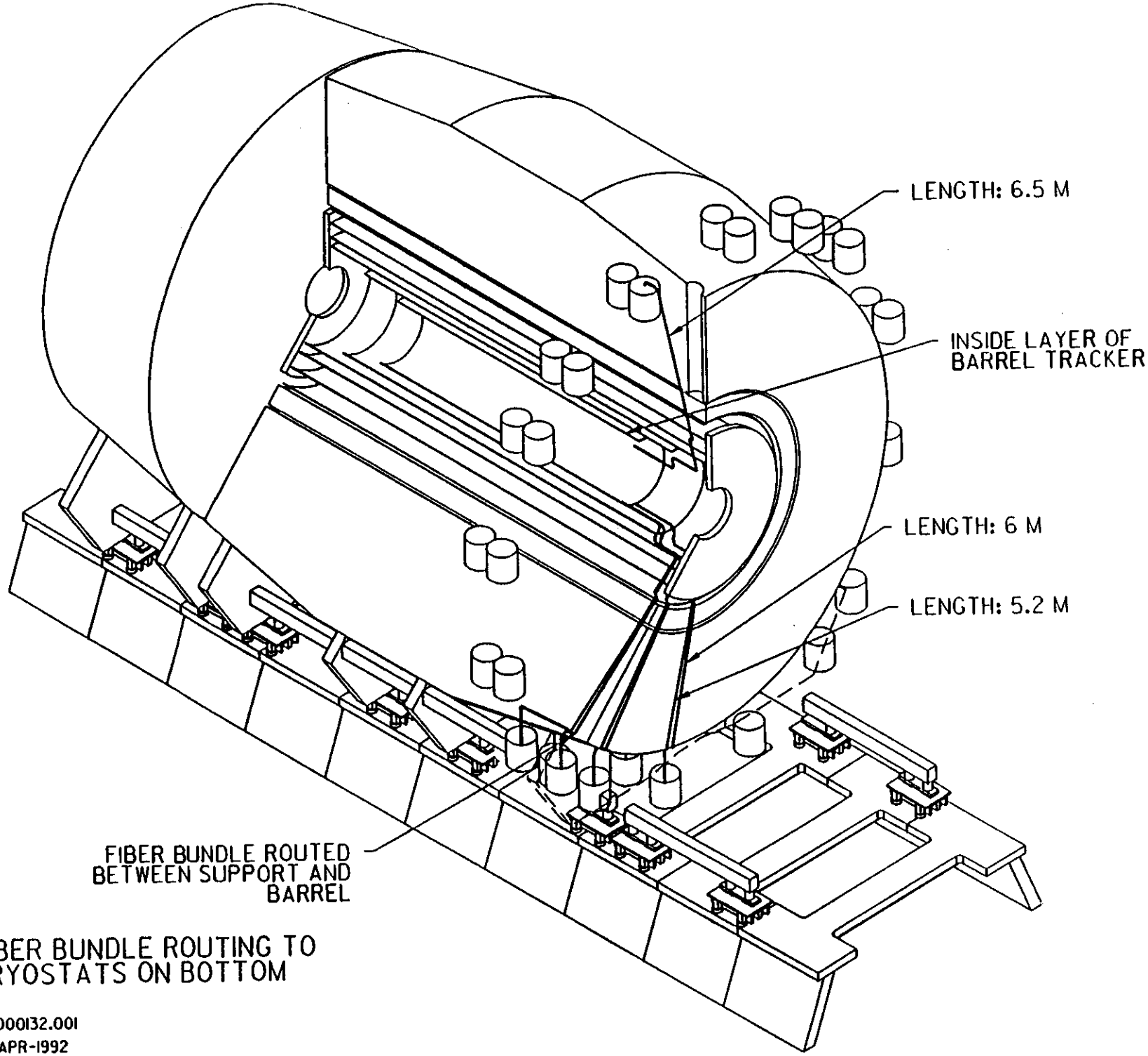

FIBER BUNDLE ROUTING TO CRYOSTATS ON BOTTOM

SDD00132.001
01-APR-1992

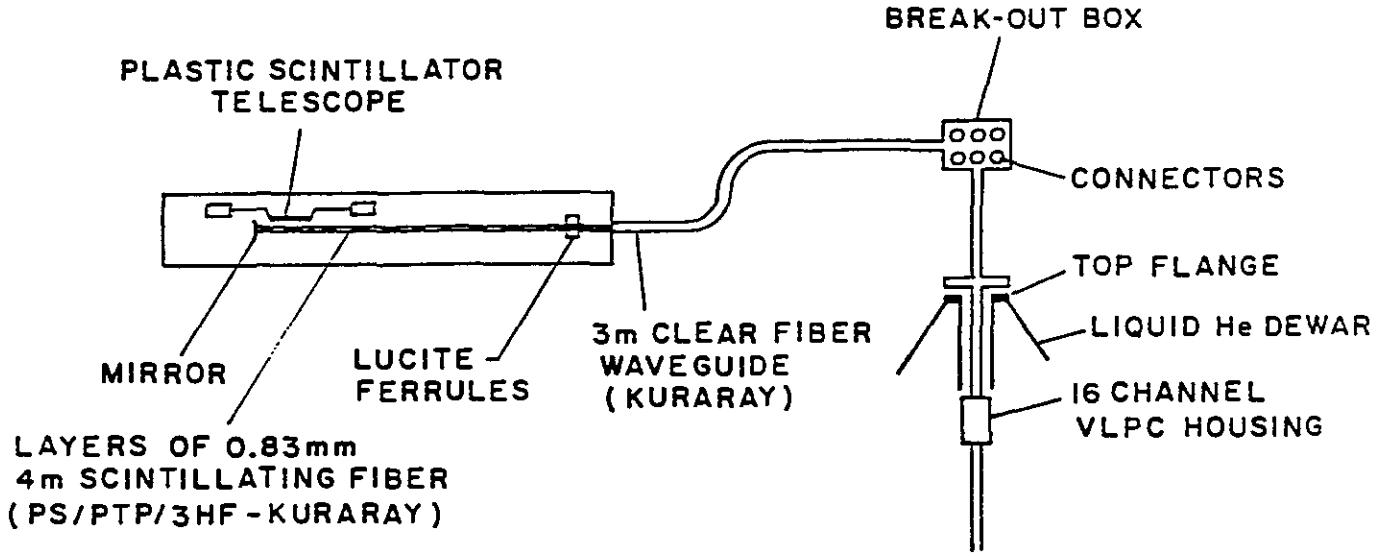
BREAK-OUT BOX
PLASTIC SCINTILLATOR
TELESCOPE
CONNECTORS
TOP FLANGE
LIQUID He DEWAR
3m CLEAR FIBER
WAVEGUIDE
(KURARAY)
MIRROR
LUCITE
FERRULES
16 CHANNEL
VLPC HOUSING
LAYERS OF 0.83mm
4m SCINTILLATING FIBER
(PS/PTP/3HF-KURARAY)

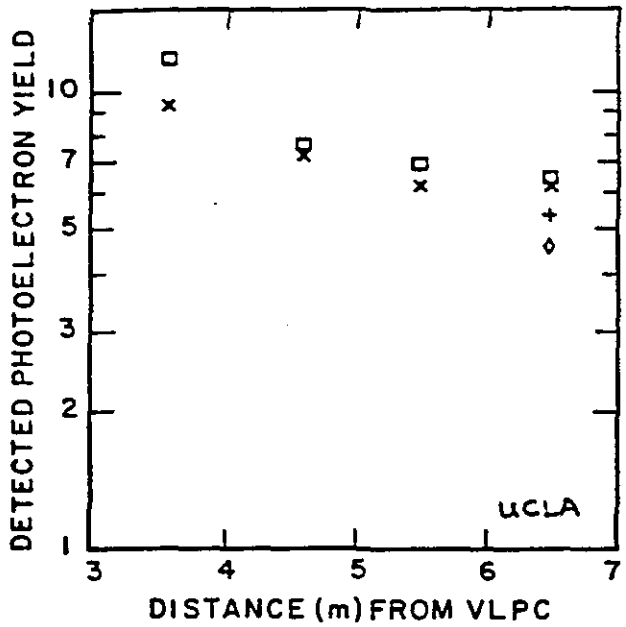

DISTANCE = 3m CLEAR WAVEGUIDE

SPLICED TO A SCINTILLATING FIBER

DIAMETER 830μm

PS/PTP/3HF (KURARAY)

□ × } MIRRORED END

+ ◇ } UNMIRRORED END

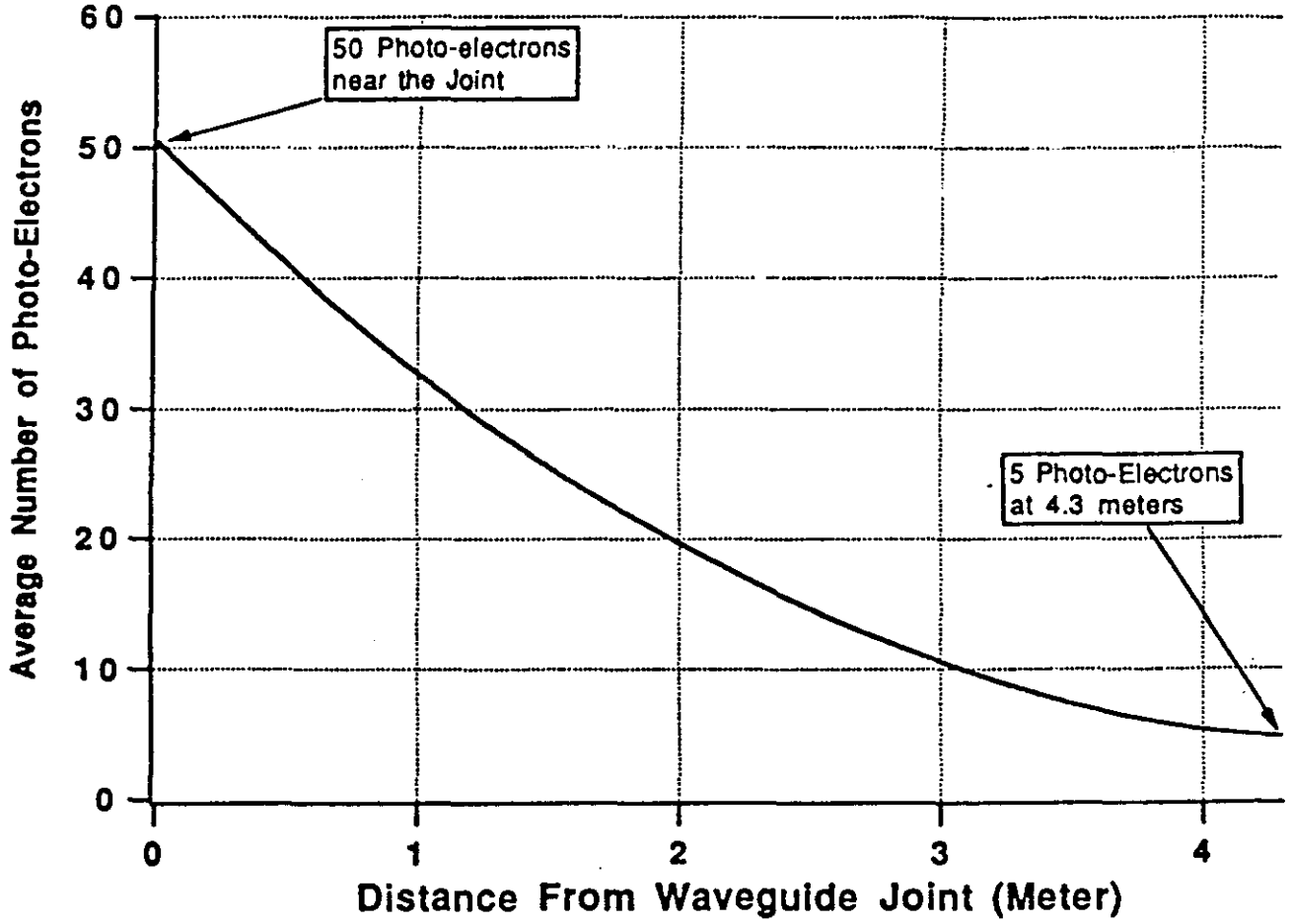

Figure 5.3.3-1 Mean detected photoelectron yield as a function of position along a scintillating fiber in layer B3 of the tracker

FOR A FIBER DOUBLET 92.5 μm DIAMETER

9.0 μm PITCH

$\langle n_{p.e.} \rangle$	EFFICIENCY	σ
1.6	0.87	170 μm
2.4	0.95	
3.2	0.98	130 μm
4.0	0.99	
4.8	0.995	115 μm

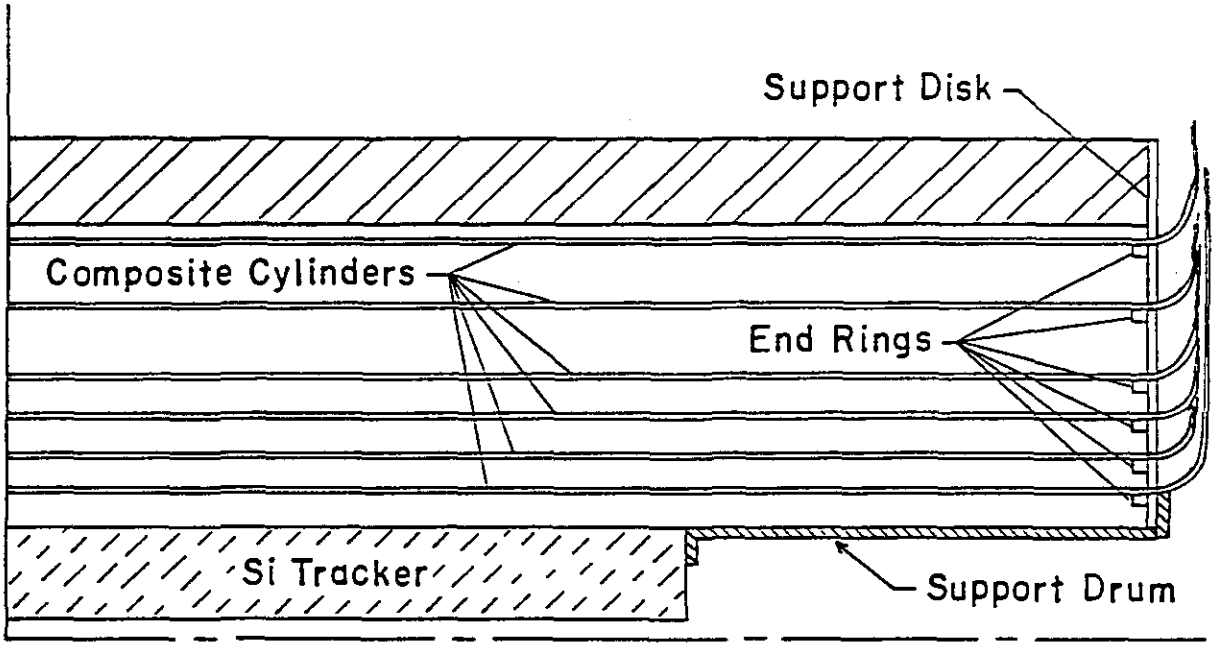
Support Disk
Composite Cylinders
End Rings
Si Tracker
Support Drum

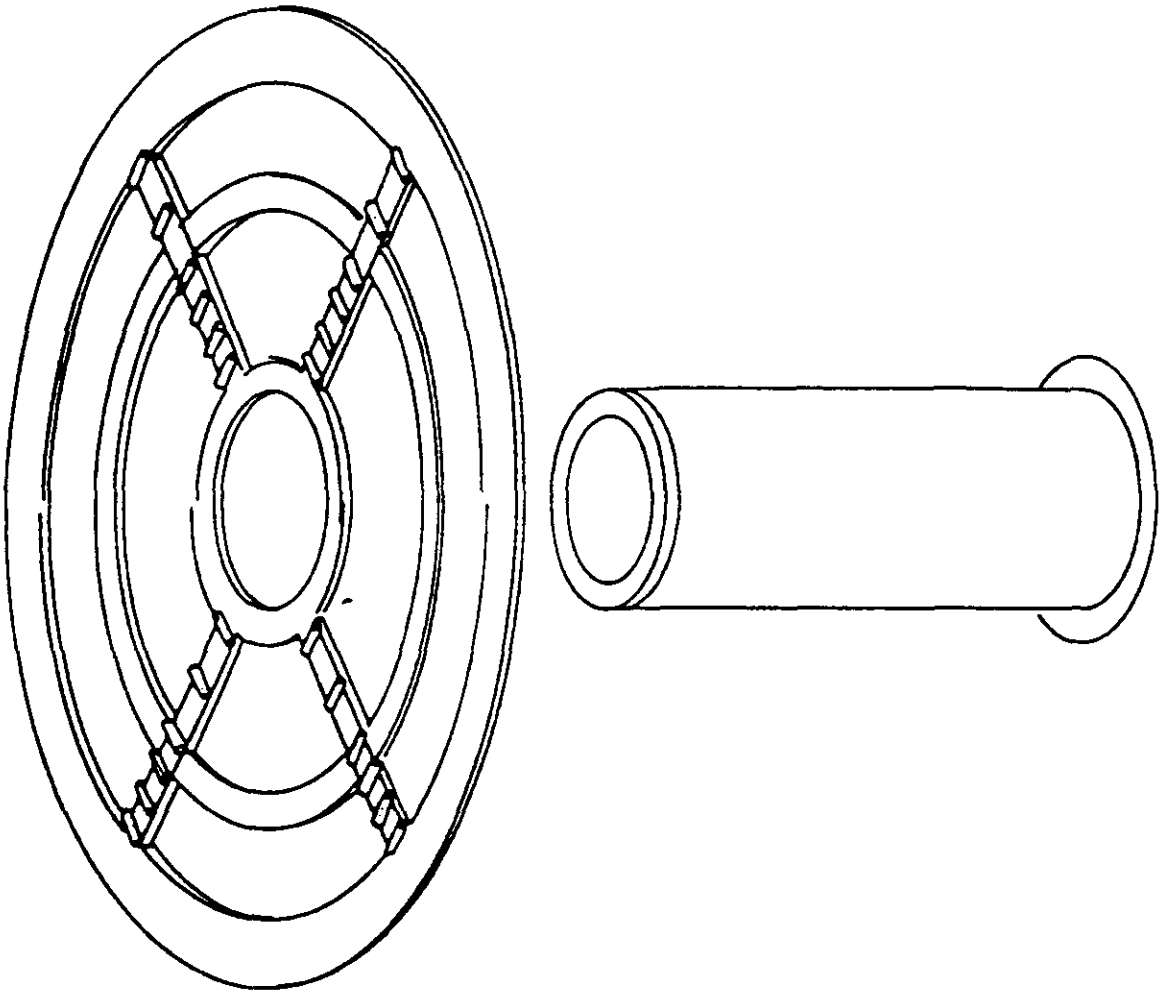

Figure 4.2-2 a.) the simple thin panel forms the backbone of the tracking system. b) The nose which connects to the silicon system to the outer tracking system.

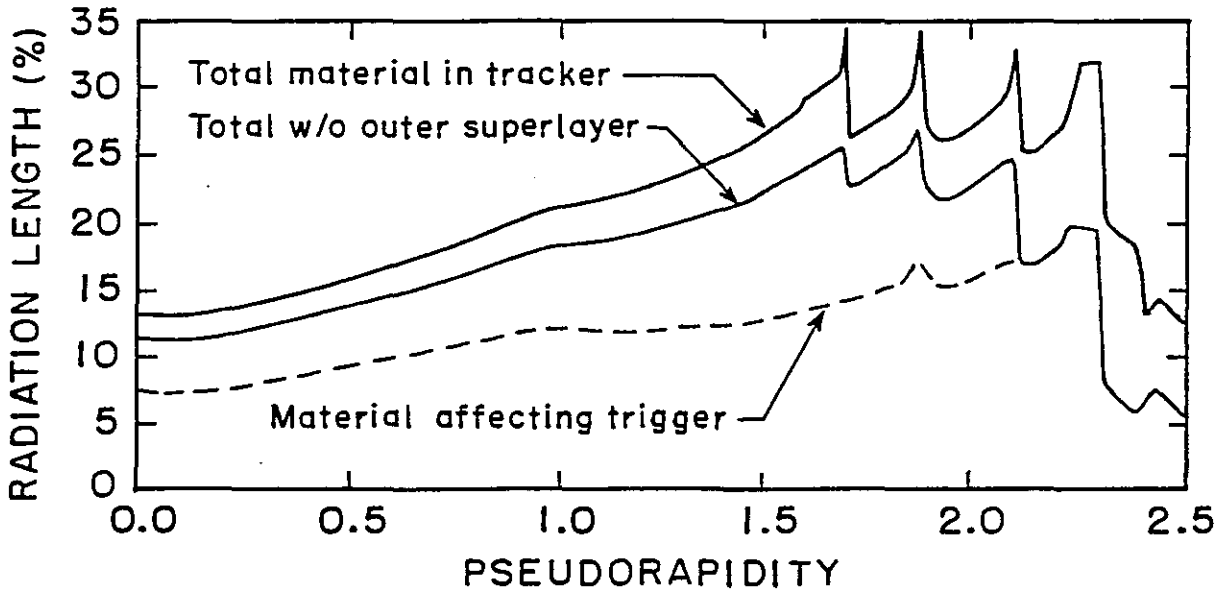
RADIATION LENGTH (%)
35
30
25
20
15
10
5
0
Total material in tracker
Total w/o outer superlayer
Material affecting trigger
0.0
0.5
1.0
1.5
2.0
2.5
PSEUDORAPIDITY

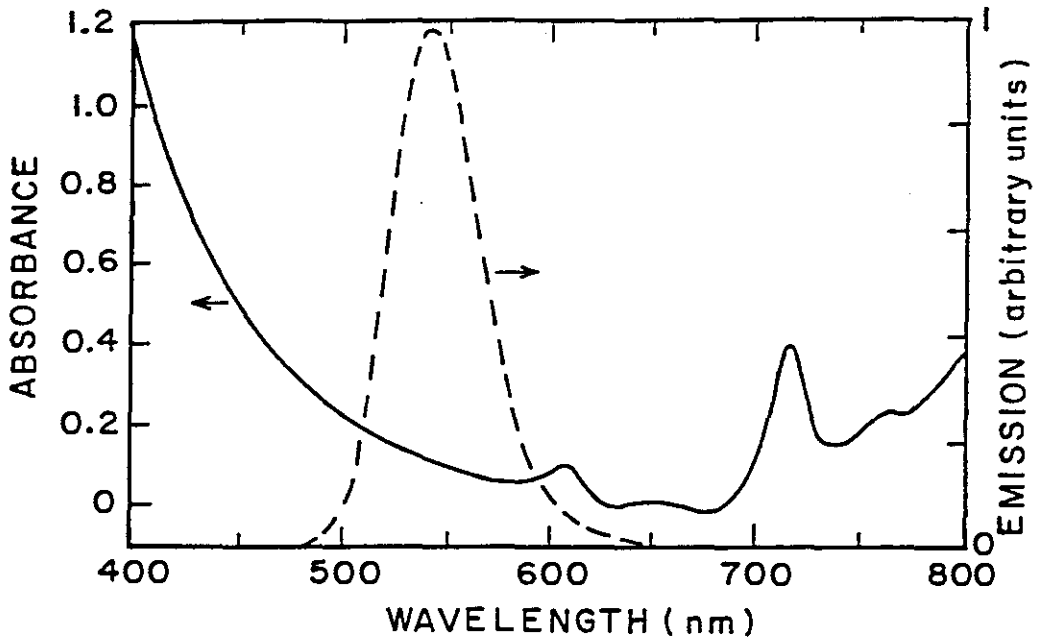
1.2
1.0
0.8
0.6
0.4
0.2
0
ABSORBANCE
1
0
EMISSION (arbitrary units)
400
500
600
700
800
WAVELENGTH (nm)

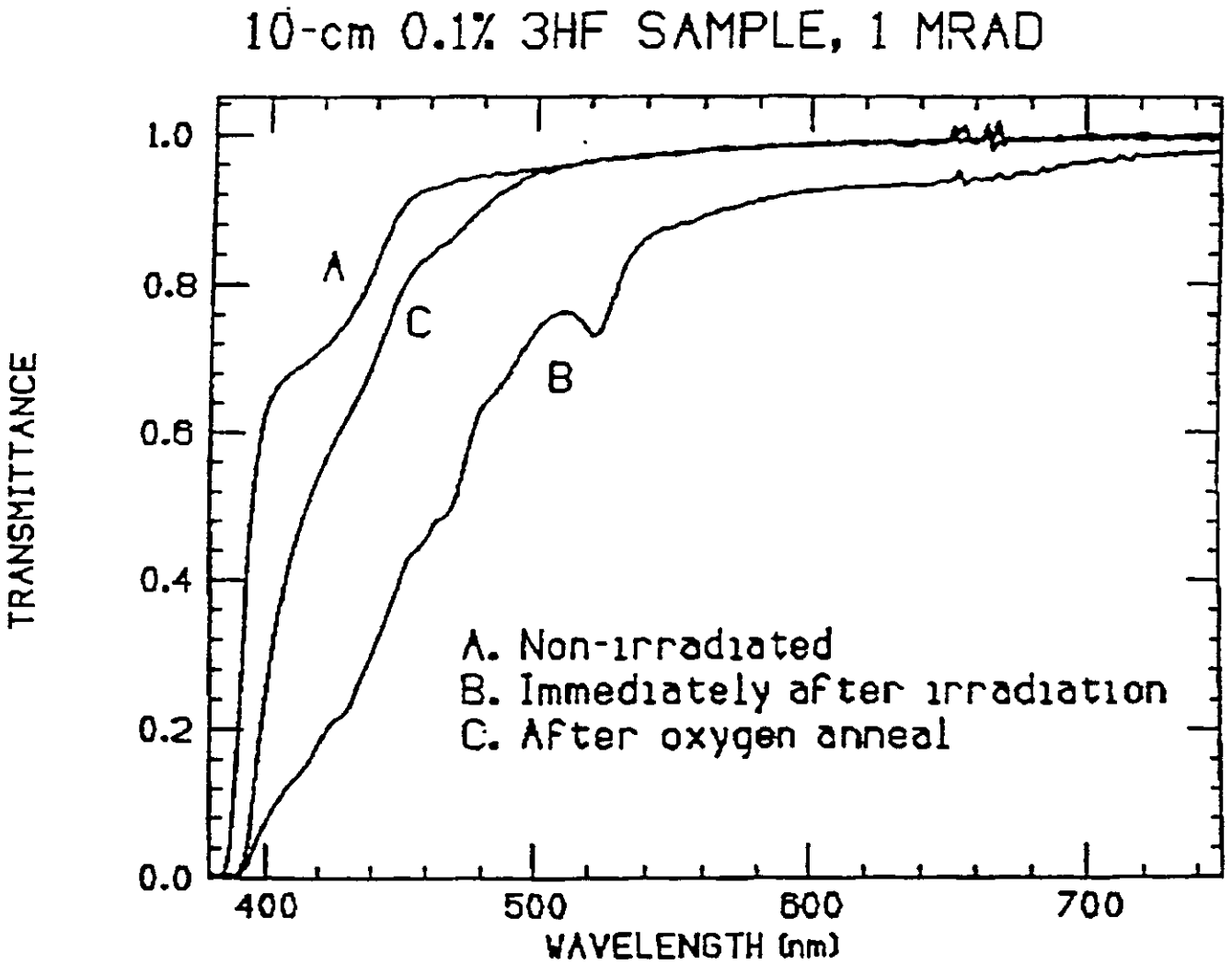

Figure 5.2-1 Transmission in polystyrene/PTP/3HF scintillator as a function of wavelength. Before and after irradiation by ^{60}Co to 1 MRad, and after annealing.

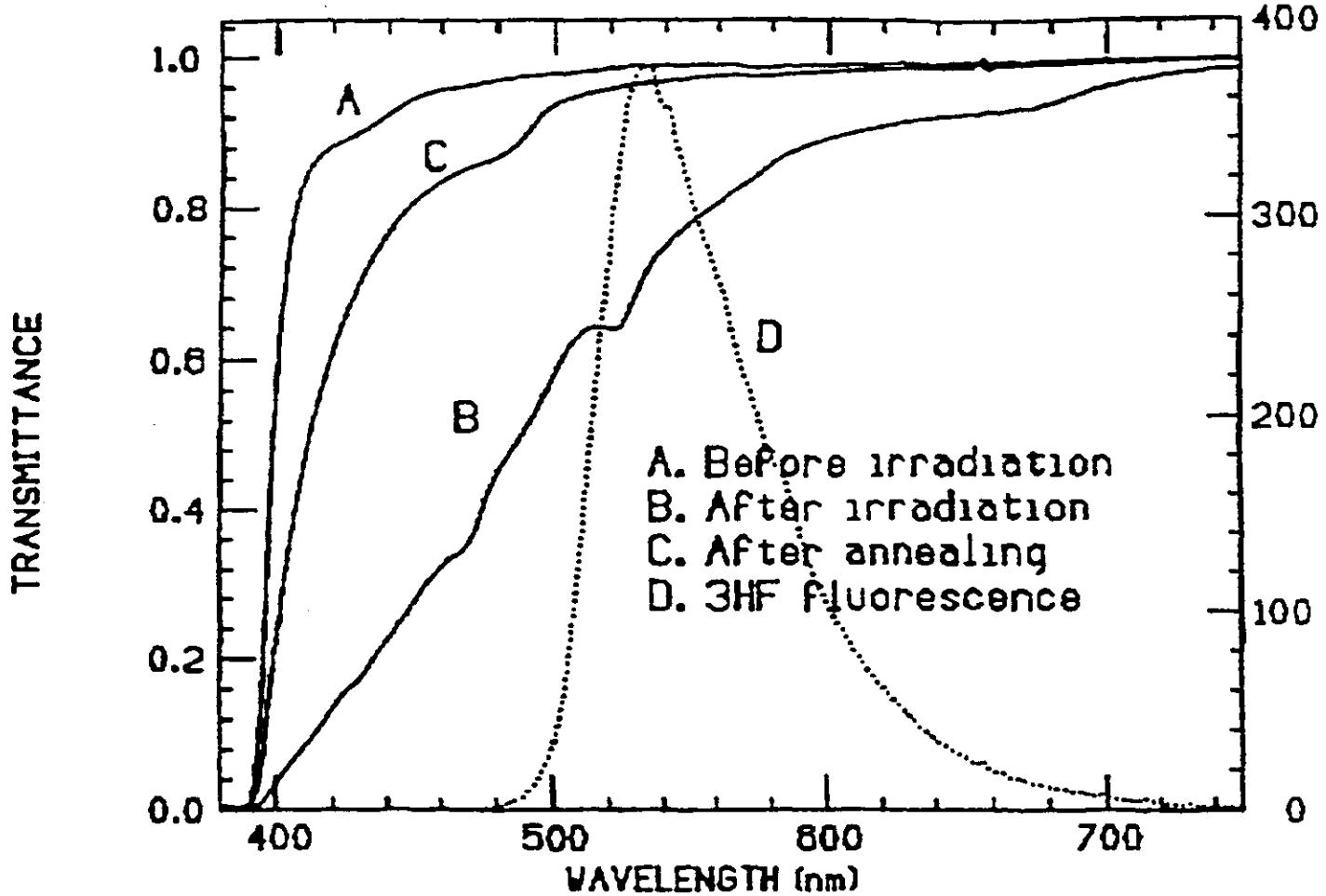

Figure 5.2-2 Transmission in polystyrene/PTP/3HF scintillator as a function of wavelength. Before and after irradiation by ^{60}Co to 10 MRad, and after annealing.

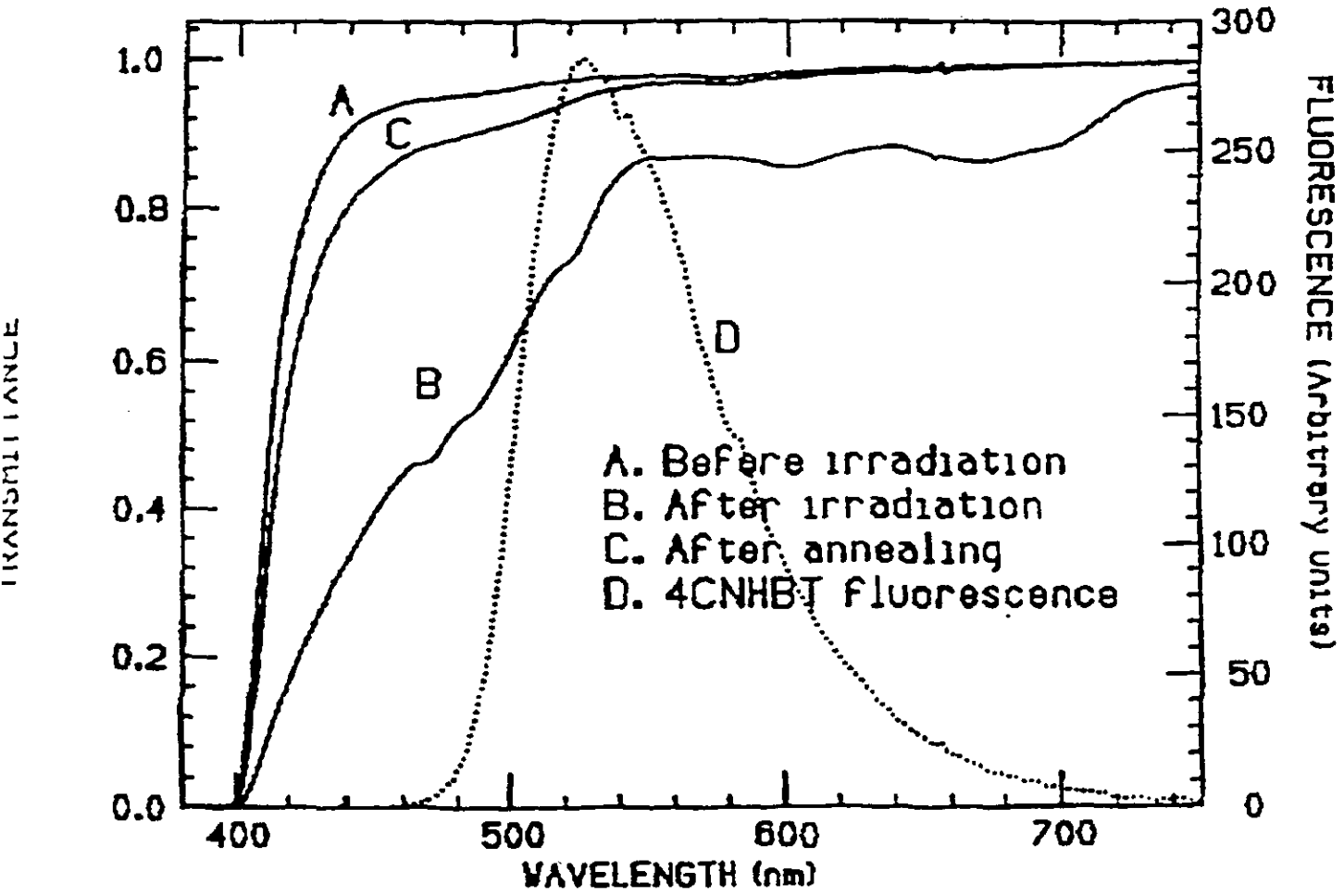

Figure 5.2-3 Transmission in polystyrene/PTP/4CNHBT scintillator as a function of wavelength. Before and after irradiation by ^{60}Co to 10 MRad, and after annealing.

RESULTS (pT+3HF)

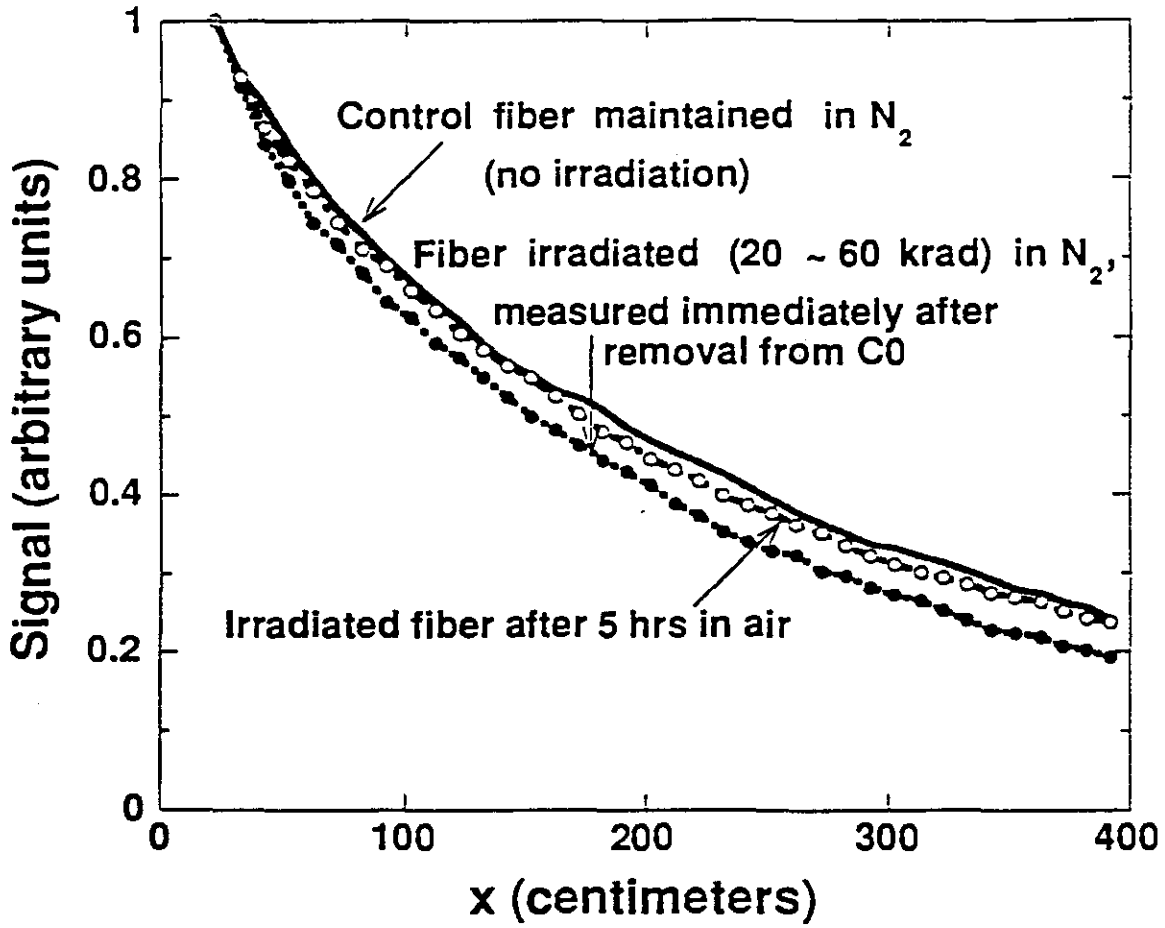

Transmission curves
(normalized to unity at x = 22 cm)

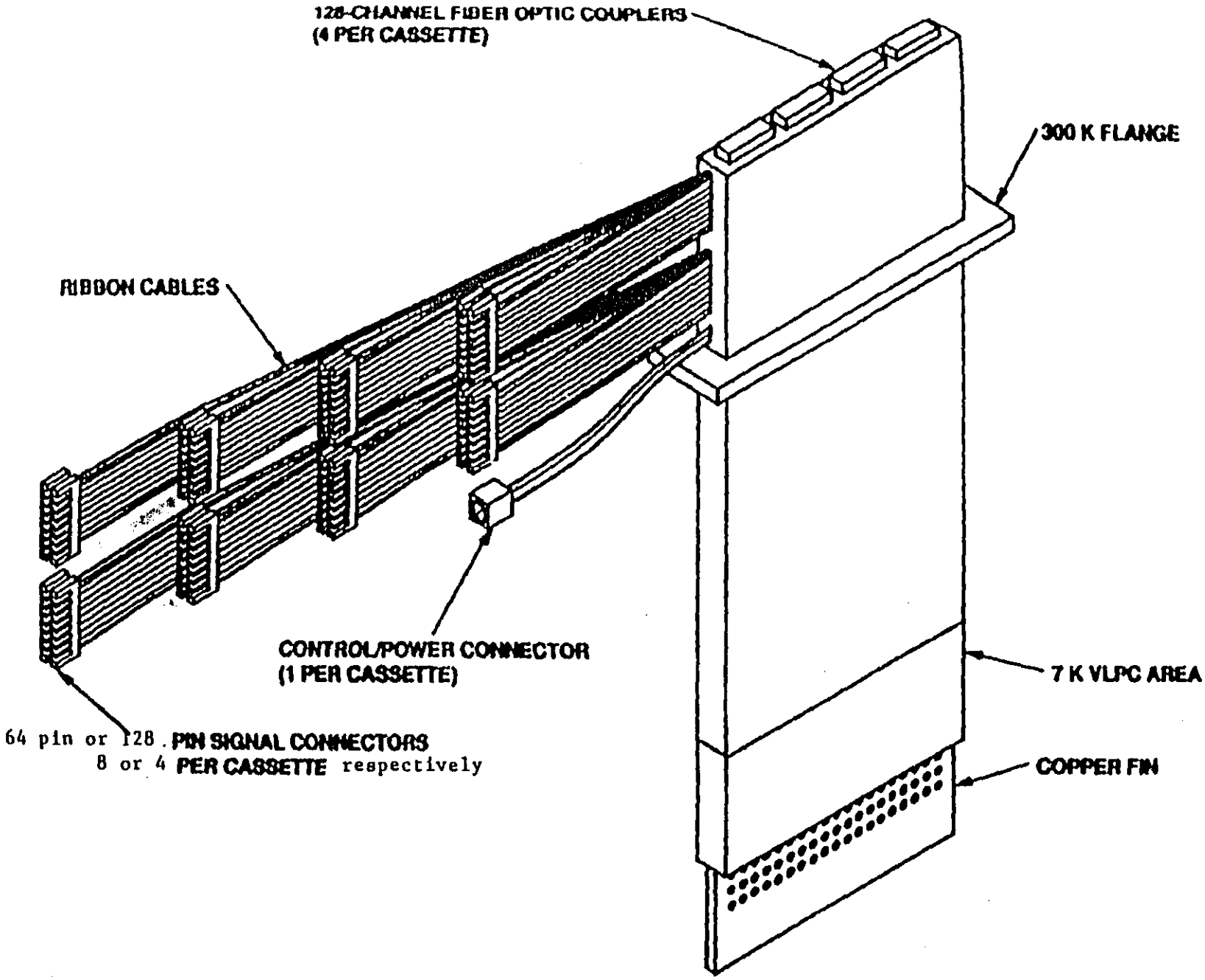
128-CHANNEL FIBER OPTIC COUPLERS
(4 PER CASSETTE)
300 K FLANGE
RIBBON CABLES
CONTROL/POWER CONNECTOR
(1 PER CASSETTE)
7 K VLPC AREA
64 pin or 128 PIN SIGNAL CONNECTORS
8 or 4 PER CASSETTE respectively
COPPER FIN

8192 CHANNEL RYOSTAT
BASELINE DESIGN

DIMENSIONS: 19 IN. DIA. x 20 IN. HIGH
(48.3 CM DIA. x 50.8 CM HIGH)

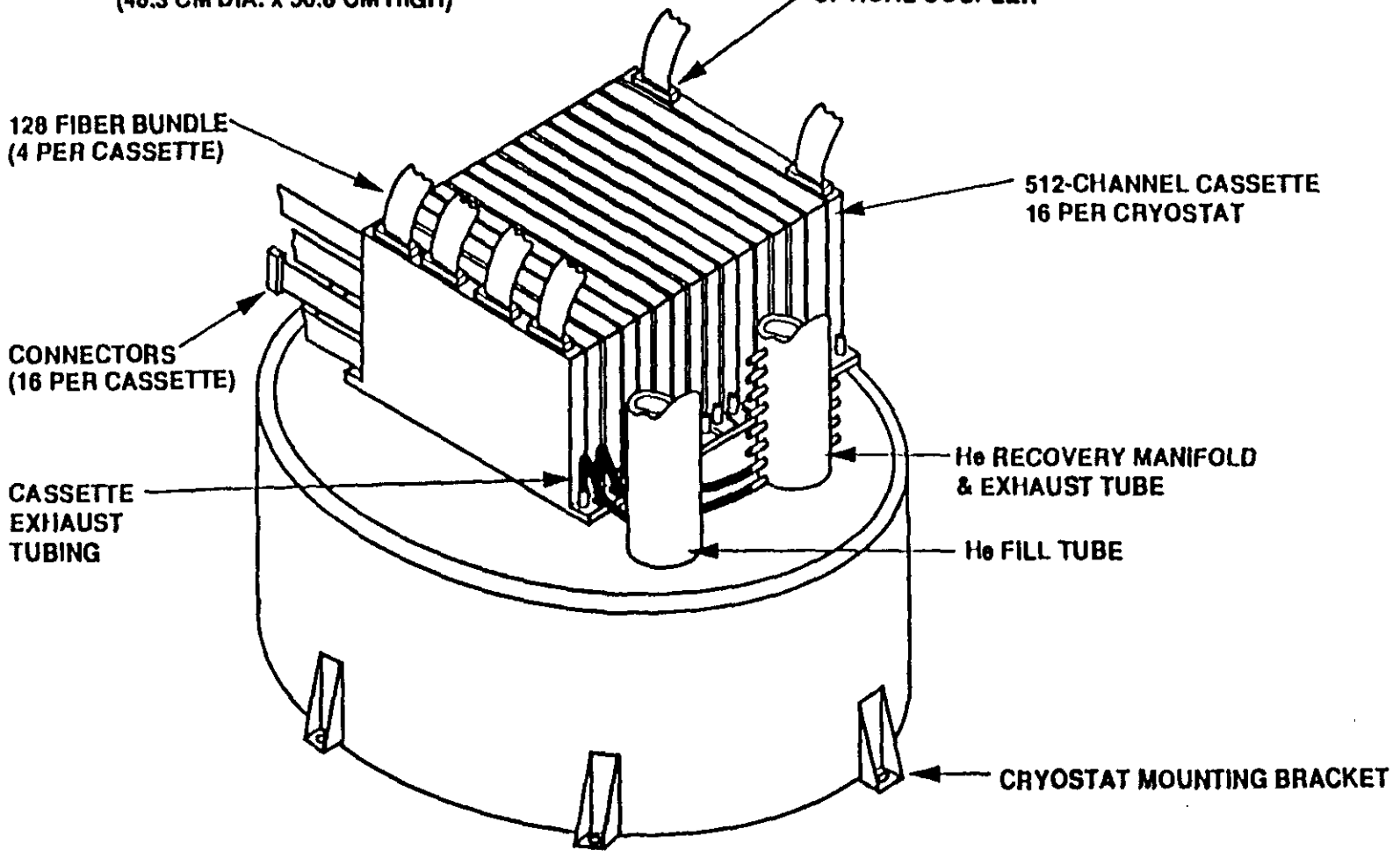

Rockwell International

8-ELEMENT VLPC ARRAY

Rockwell International Science Center

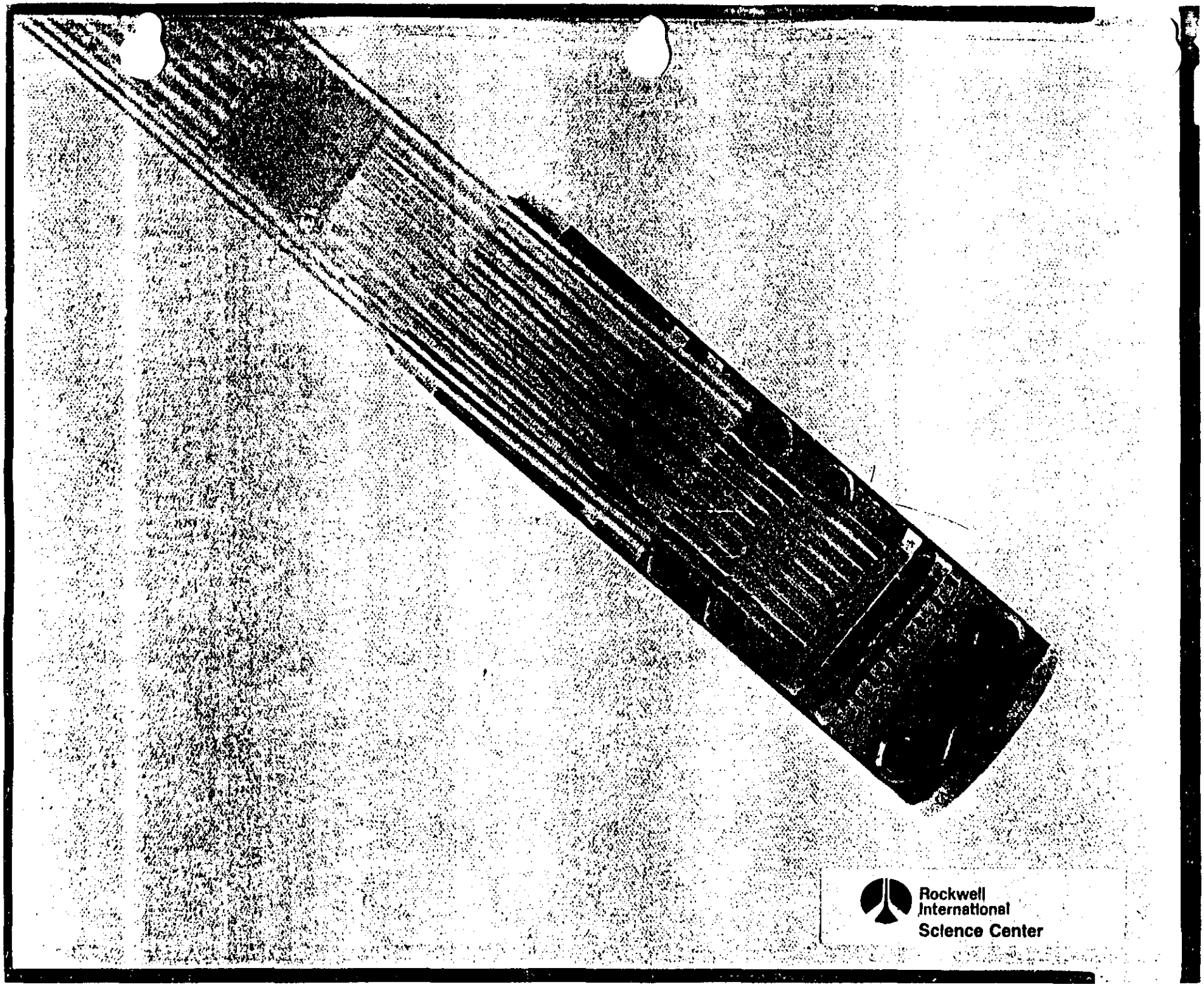
Rockwell
International
Science Center

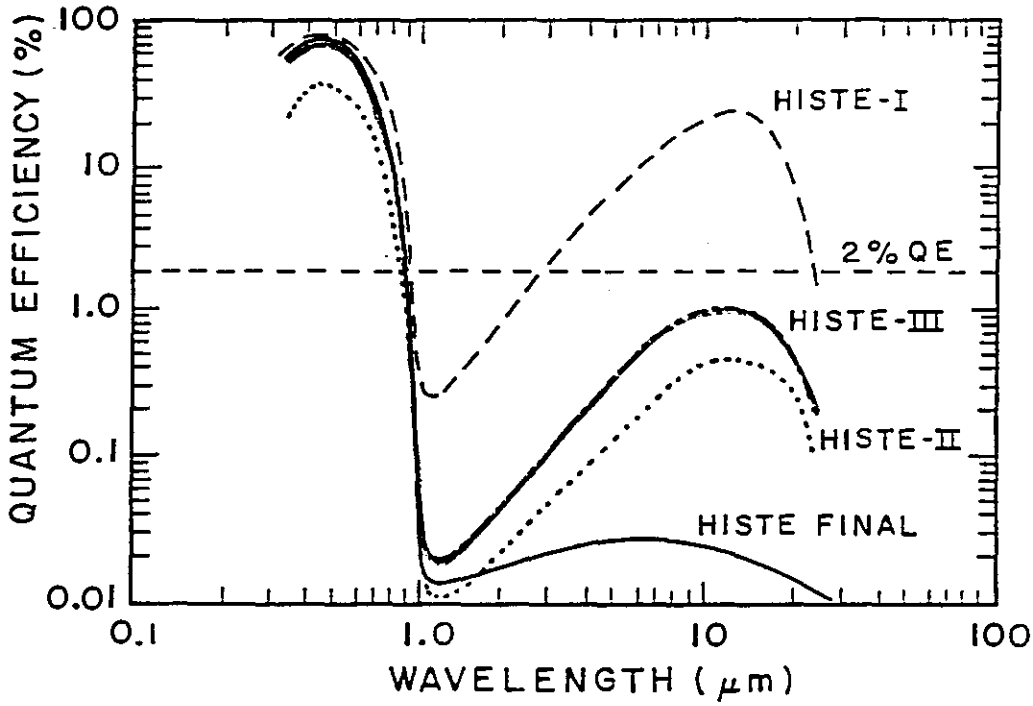
QUANTUM EFFICIENCY (%)
100
10
1.0
0.1
0.01
0.1
1.0
10
100
WAVELENGTH (μm)
HISTE-I
2% QE
HISTE-III
HISTE-II
HISTE FINAL

Table 4-24
Geometric and operating characteristics of visible light photon counters.

Parameter	Achieved	Goal
Active area	$875 \times 875\ \mu m^2$	1 mm diameter
Array configuration	1×8	1×10
Contact resistance	1000 Ω	<100 Ω
Pulse rise time	< 5 ns	< 5 ns
Average gain	20,000	30,000
Gain dispersion	< 30%	< 30%
Effective QE at 565 nm	85%	70–90%
Infrared QE at 15	< 0.5%	< 2%
Dead time	None (continuous)	None (continuous)
After pulses	< 0.01%	< 0.01%
Dark pulse rate	10 kHz	5 kHz
Saturation pulse rate	25 MHz	25 MHz
Average current	< 200 nA	< 200 nA
Average power	1.4 μW/channel	1.6 μW/channel
Breakdown voltage	7.5 V	> 8.5 V
Operating bias voltage	6–8 V	6–8 V
Neutron damage level	$> 10^{11}$ n/cm^2	$> 10^{11}$n/cm^2
Operating temperature	6–8 K	6–8 K

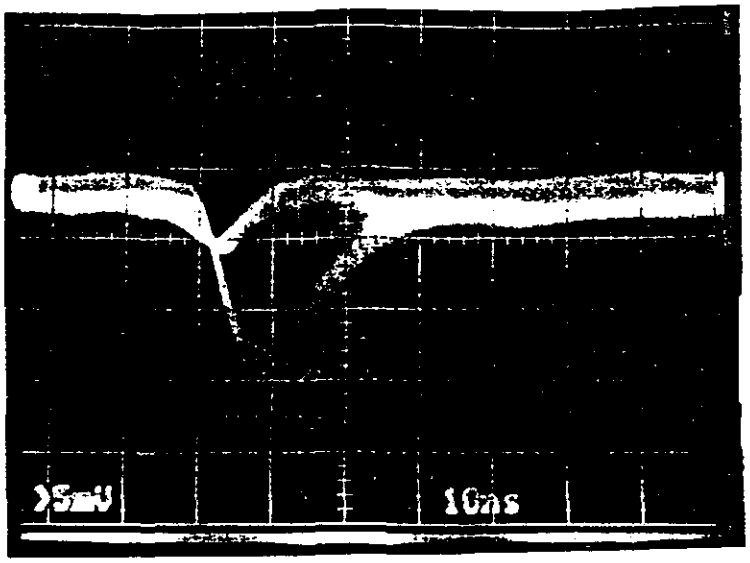

1/2/1992

Tests with HISTE-II VLPCs

Using VTX amplifiers

Bias Voltage : 7.8 volts

Temperature: 9.5 K

Looking at thermal electron pulses

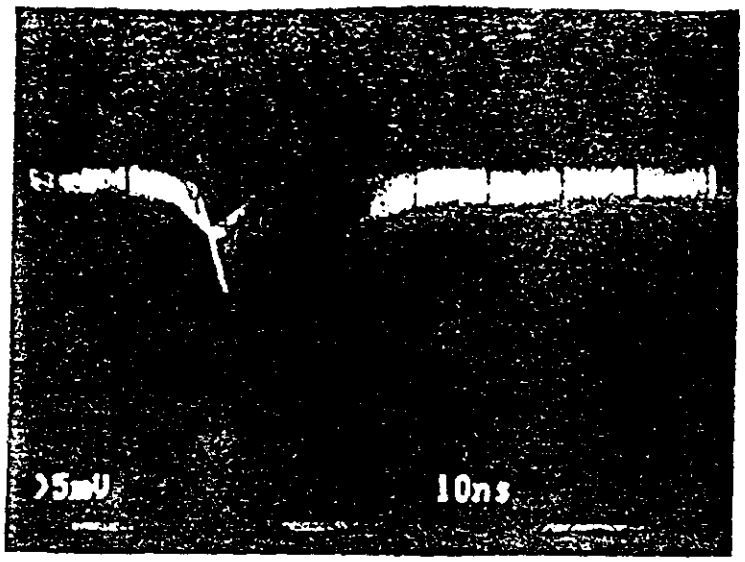

Figure 2.2-14 Typical signal from the HISTE-II/VTX system operating in the test beam at Fermilab, indicating a clear single-photoelectron line above noise and a pulse rise of less than 5ns. As displayed, the signal has received additional amplification in an LRS 612 preamplifier as was the case prior to data recording in the LRS2880 ADC system.

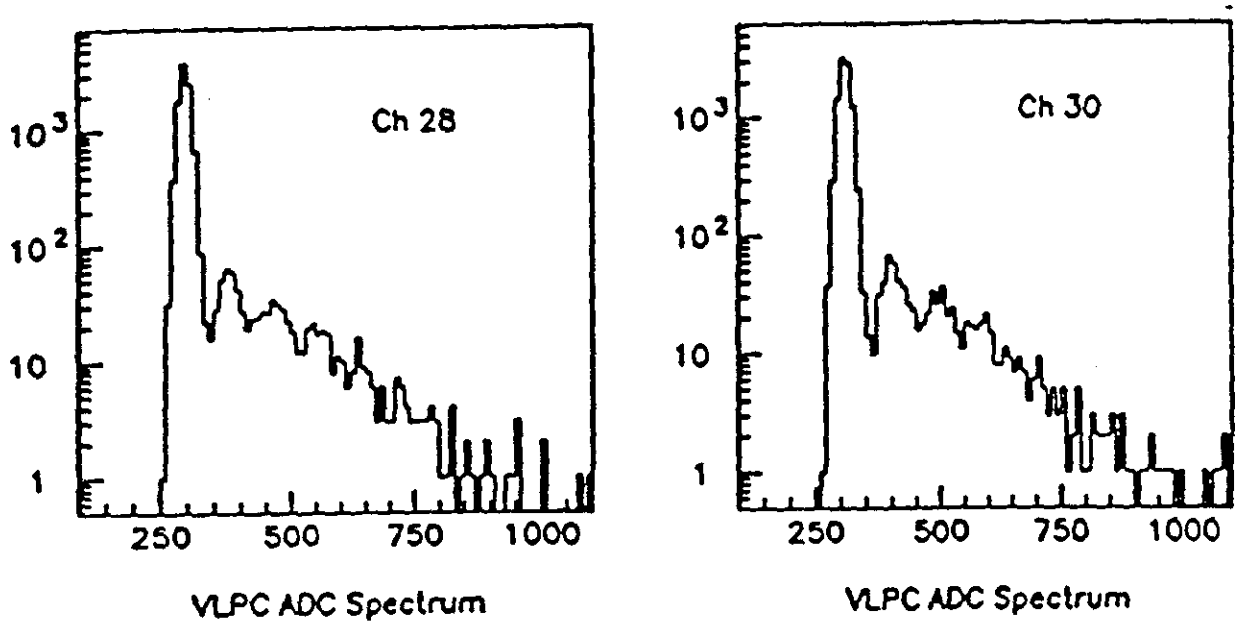

Figure 2.2-15 A typical pulse height spectrum observed in the fiber/HISTE-II/VTX system recorded during the beam tests at Fermilab and exhibiting characteristic photopeaks.

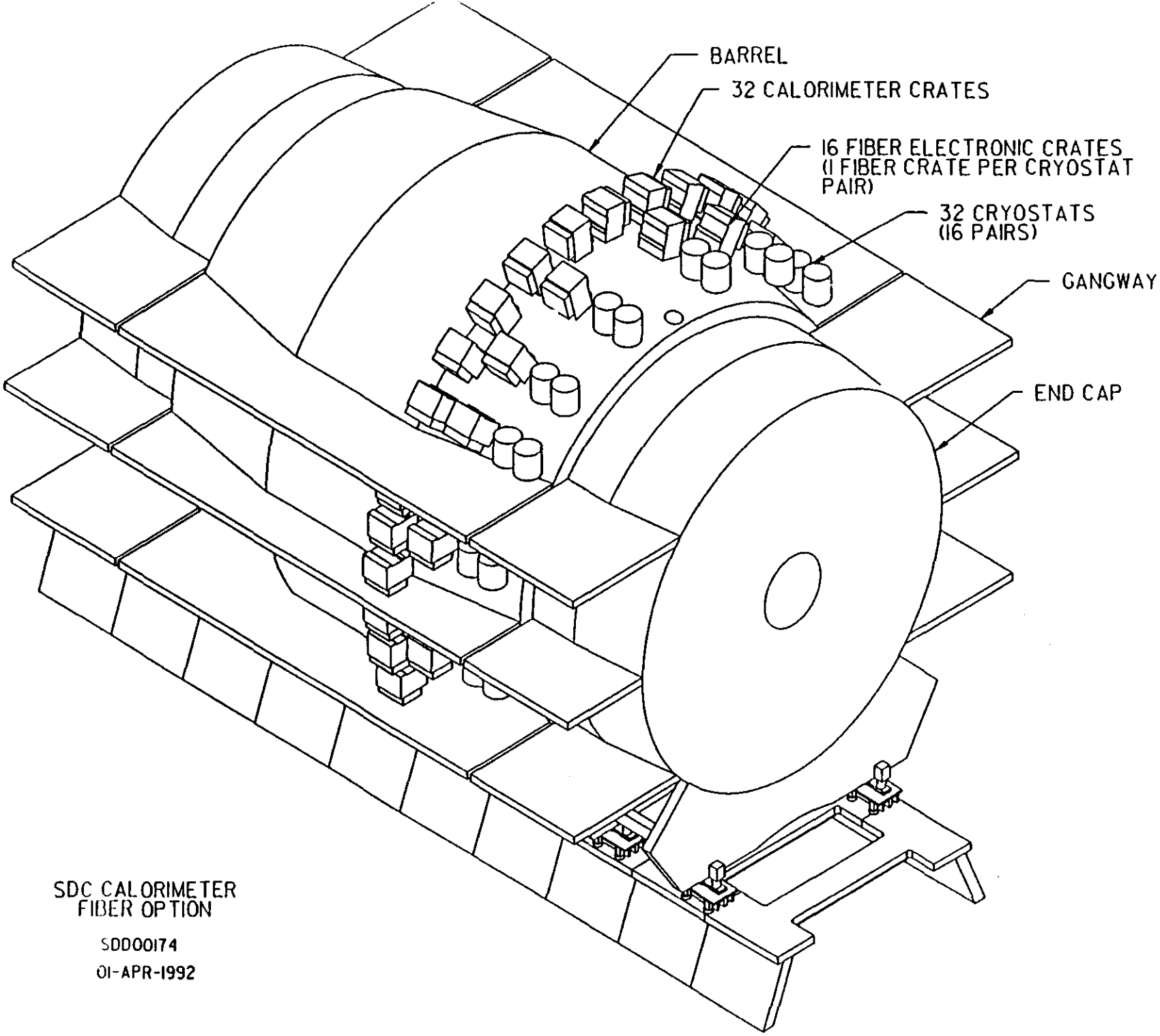

SDC CALORIMETER
FIBER OPTION

SDD00174

01-APR-1992

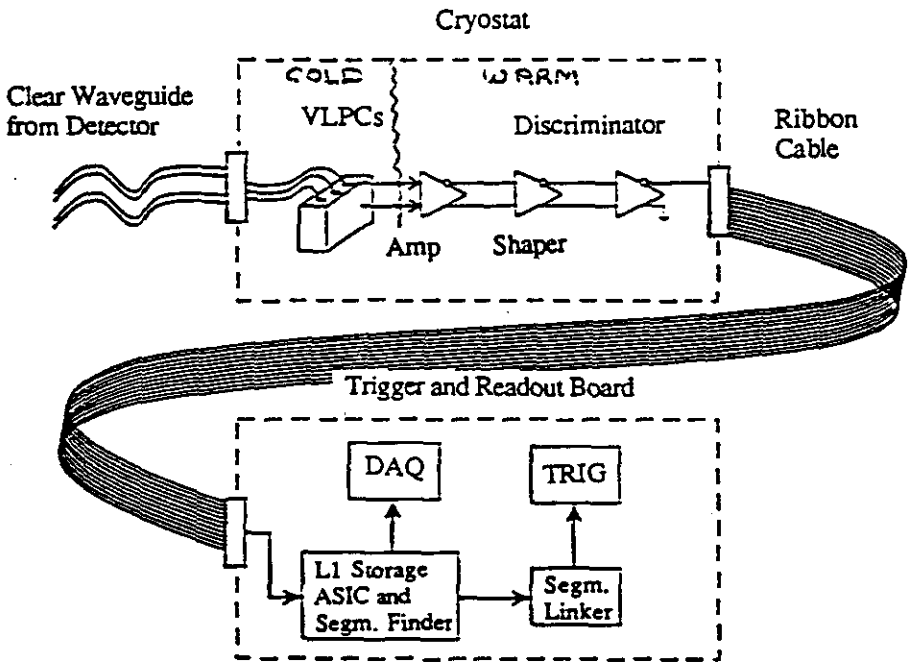
Cryostat
COLD
WARM
Clear Waveguide
from Detector
VLPCs
Discriminator
Ribbon
Cable
Amp
Shaper
Trigger and Readout Board
DAQ
TRIG
L1 Storage
ASIC and
Segm. Finder
Segm.
Linker

Track Segment Finding Algorithm

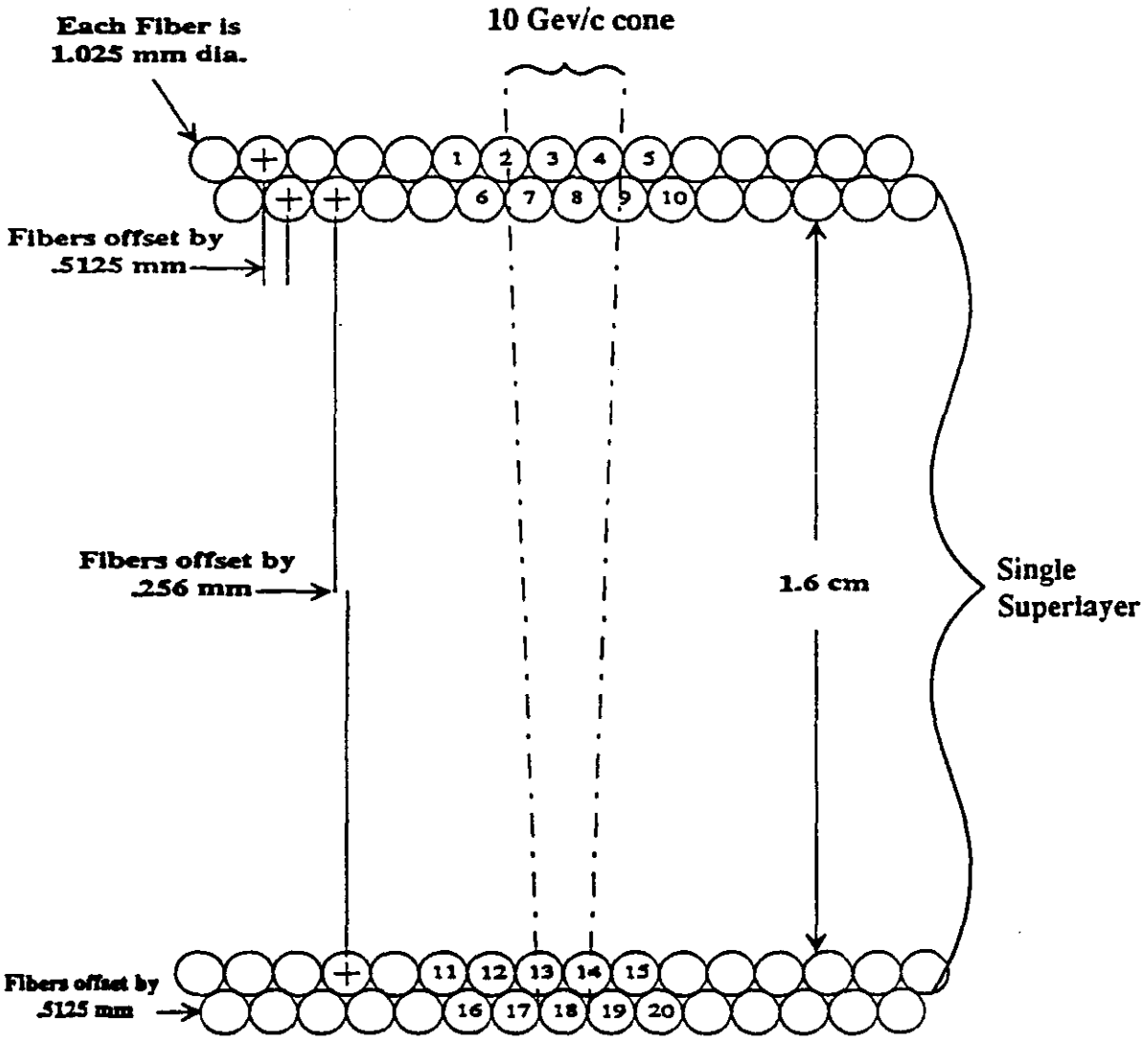

Acceptance cones for 10 GeV tracks
in single fiber bins

KLK
01/22/92

Triplet Superlayers for Trigger

Single Fiber Diameter Hit Locations

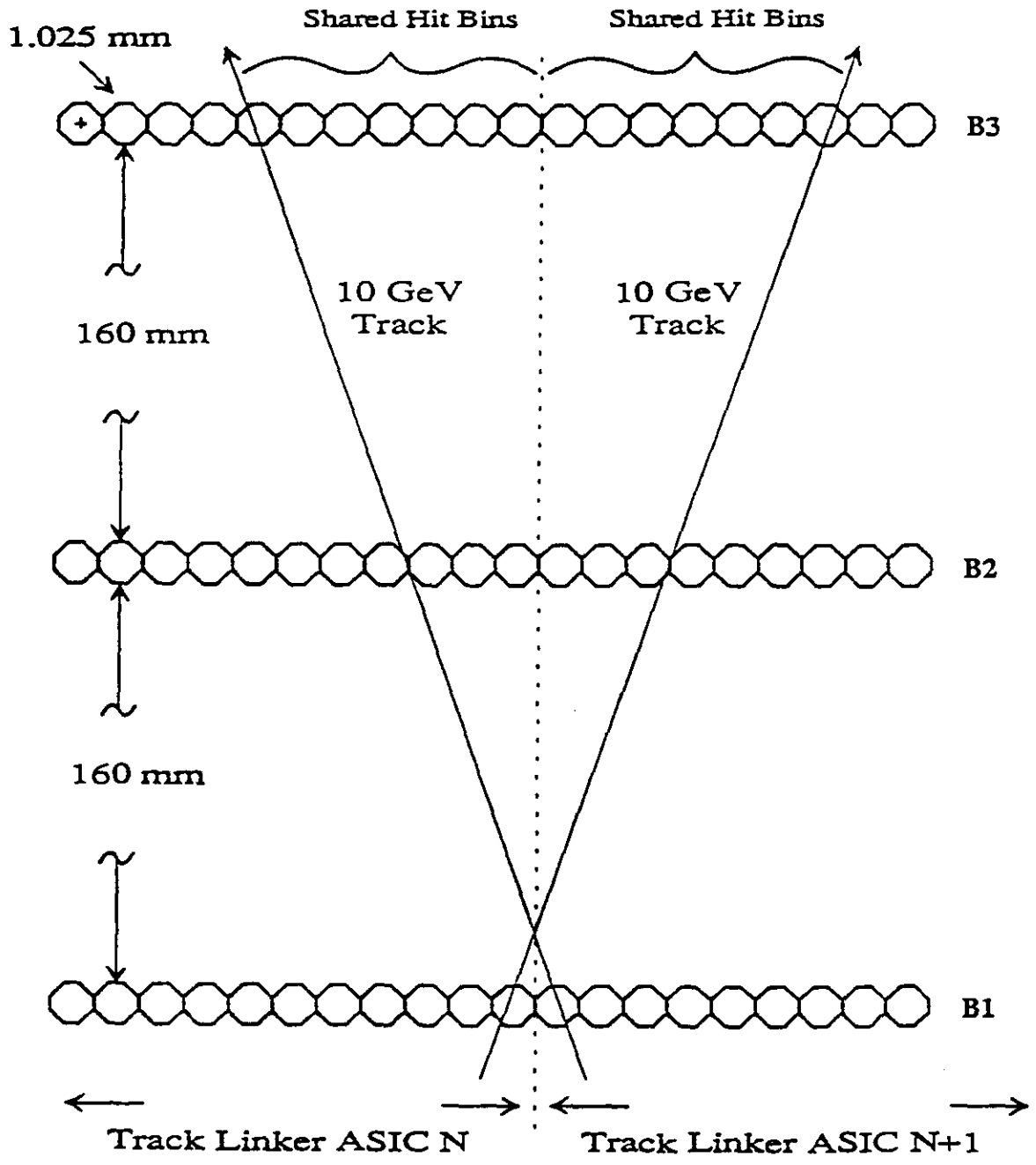

KLK
01/22/92

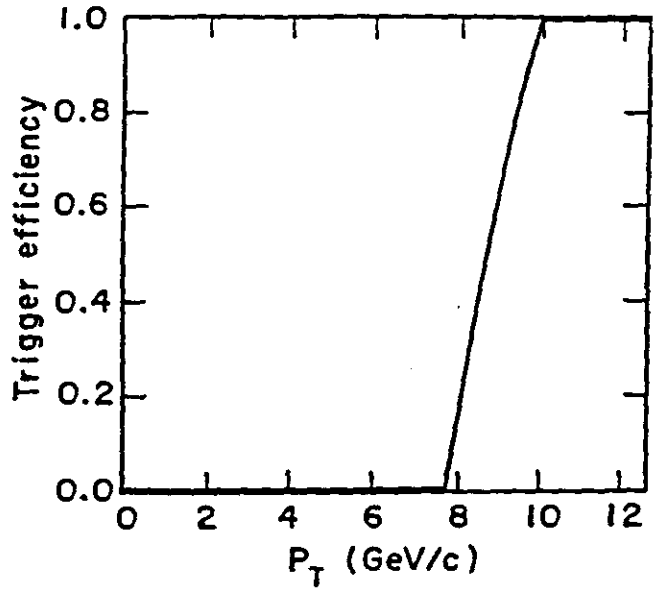

FIG. 4-64. Trigger efficiency as a function of p_t for the scintillating fiber tracking trigger using superlayers B1, B2, and B3.

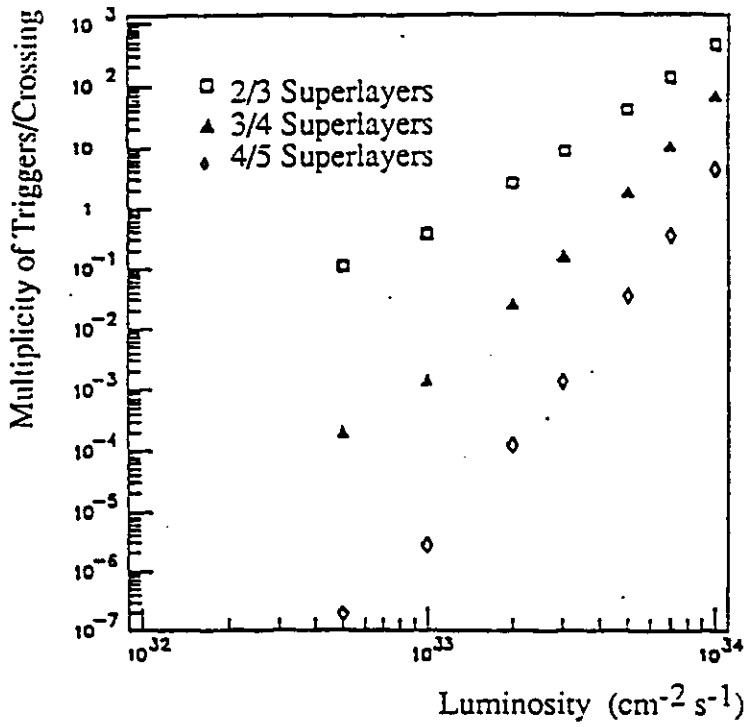
Multiplicity of Triggers/Crossing
2/3 Superlayers
3/4 Superlayers
4/5 Superlayers
Luminosity (cm-2 s-1)

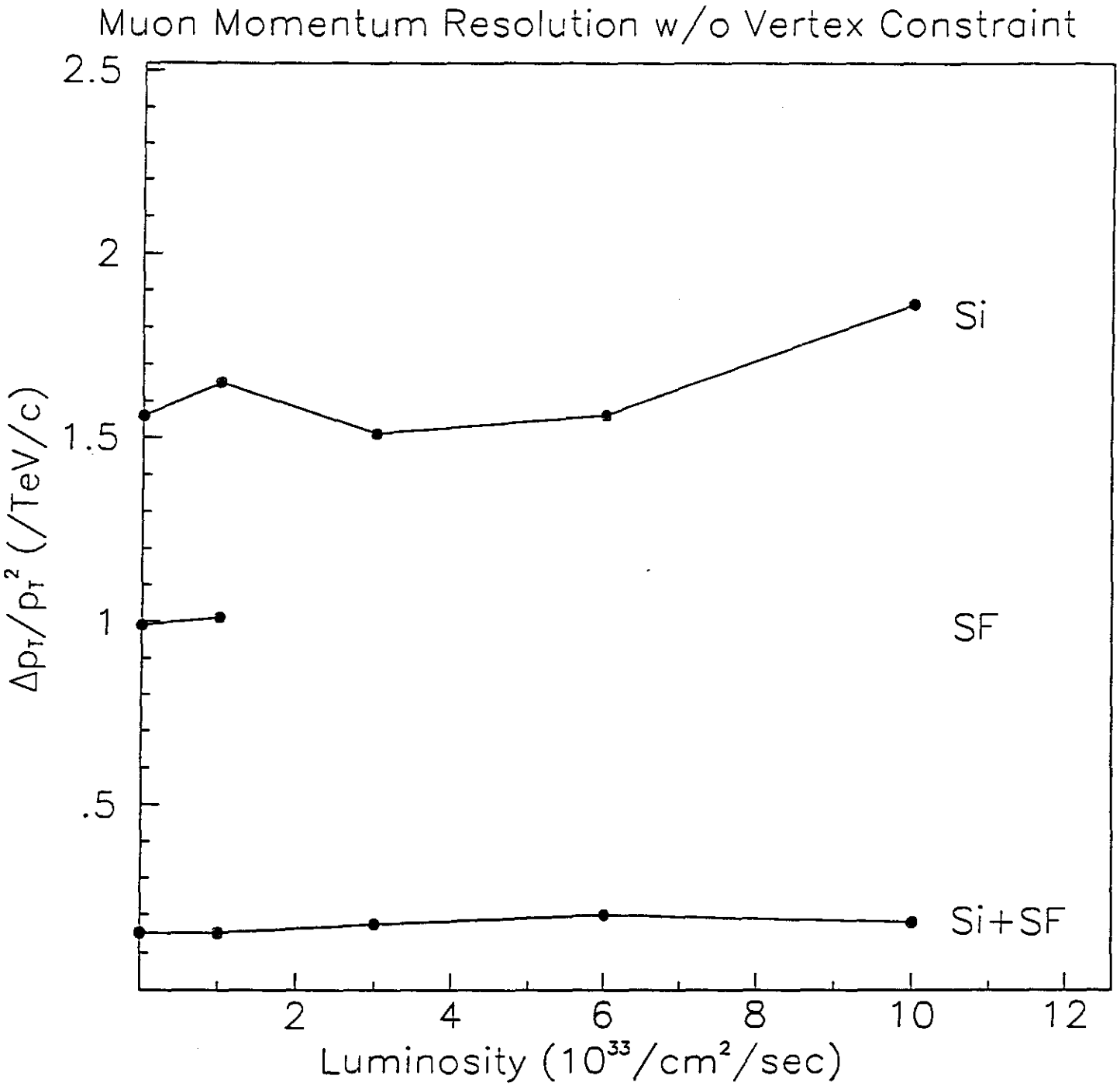
Muon Momentum Resolution w/o Vertex Constraint
2.5
2
1.5
1
.5
$\Delta p_T/p_T^2$ (/TeV/c)
Si
SF
Si+SF
2
4
6
8
10
12
Luminosity (10^{33}/cm^2/sec)

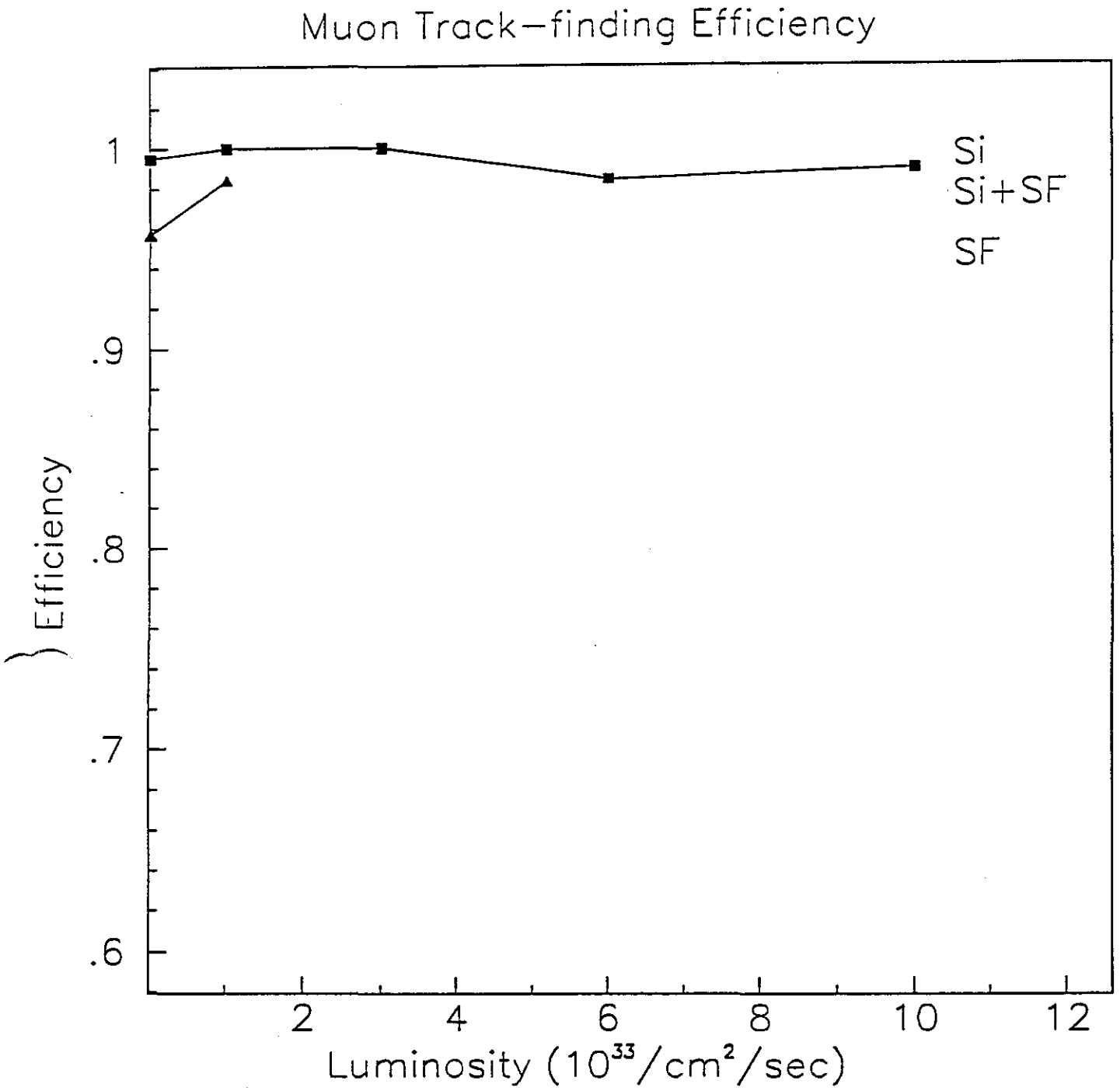
Muon Track–finding Efficiency
Si
Si+SF
SF
1
.9
.8
.7
.6
Efficiency
2
4
6
8
10
12
Luminosity ($10^{33}/cm^2/sec$)

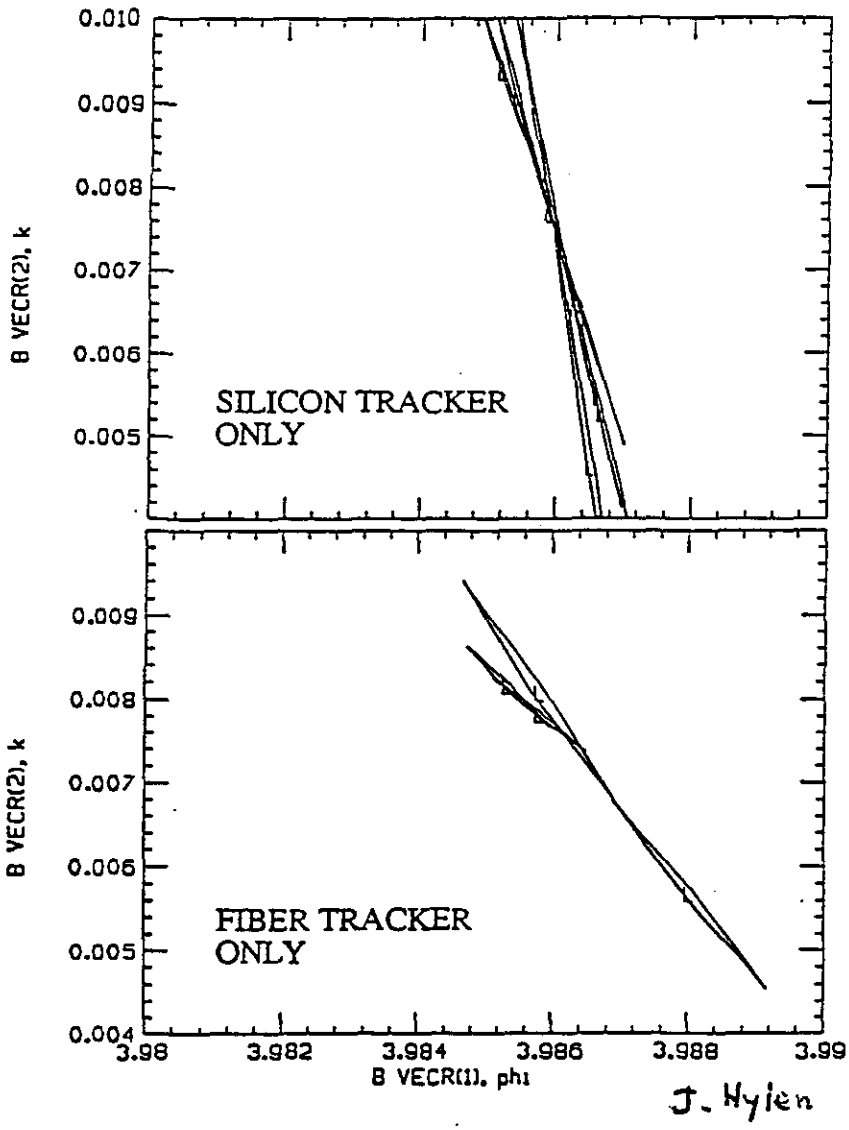
0.010
0.009
0.008
0.007
0.006
0.005
B VECR(2), k
SILICON TRACKER
ONLY
0.009
0.008
0.007
0.006
0.005
0.004
B VECR(2), k
FIBER TRACKER
ONLY
3.98
3.982
3.984
3.986
3.988
3.99
B VECR(1), phi
J. Hylen

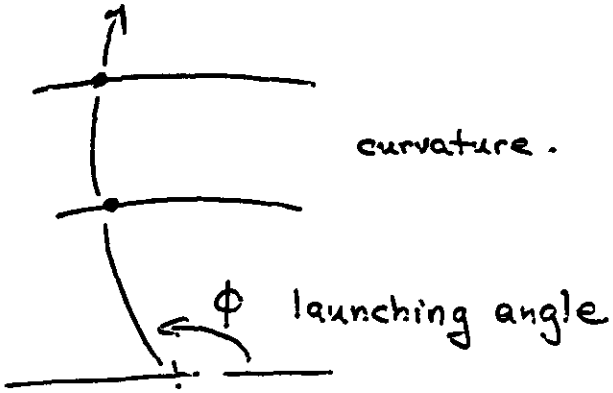
curvature.
ϕ launching angle

SUMMARY : SCINTILLATING FIBER OUTER TRACKER

1. INTRINSICALLY PROMPT RESPONSE

2. LOW OCCUPANCY

3. $|\eta| < 2.3$ COVERAGE WITH CYLINDRICAL GEOMETRY

   NO CRACKS
   MECHANICAL SIMPLICITY
   LOWER COST

4. READOUT & ELECTRONICS OUTSIDE TRACKING VOLUME

   ACCESS EASE
   NO POWER DISSIPATION IN TRACKING VOLUME.

5. DIGITAL OUTPUT

6. LEVEL 1 TRIGGERING

CHALLENGES

1. CRYOGENIC COOLING FOR PHOTODETECTORS

2. SCINTILLATOR PERFORMANCE

   RADIATION
   ENVIRONMENT

3. RIBBON & CYLINDER FABRICATION

   PLACEMENT
   STABILITY
   MONITORING